Stochastic modeling of the turbulent subgrid fluid velocity along inertial particle trajectories

By P. Fede†, O. Simonin‡, P. Villedieu† AND K. D. Squires¶

Large Eddy Simulation (LES) coupled with discrete particle simulation (DPS) has emerged as a powerful tool for the numerical prediction of particle dynamics in turbulent flows. To further advance the technique, several issues require investigation. These include, for the fluid phase, the effect of the particles on subgrid-scale fluid turbulence, and for the particulate phase, the effect of the subgrid fluid turbulence on particle dispersion and inter-particle collision rates. The present study focuses on the modeling of the subgrid fluid velocity fluctuations along inertial particle trajectories. The focus of this work is particles with relaxation times close to the subgrid turbulent time scale of the fluid. A Langevin model has been derived that ensures that the resulting equation for the variance of the subgrid velocity along particle paths is consistent with the mean subgrid kinetic energy equation derived from the filtered Navier-Stokes system. To assess the model, one- and two-point statistics measured from discrete particle simulations using fluid velocity fields computed using DNS of homogeneous isotropic turbulence are compared with results obtained using filtered velocity fields (obtained from the DNS ones) and the stochastic Langevin equation for the subgrid velocity reconstruction. The results show that the stochastic subgrid model enables accurate prediction of the particle kinetic energy, with a reasonable match to the DNS database. In contrast, the PDF of the particle concentration undergoes relatively stronger modifications due to the incorporation of the model, with the simulations showing that the random contribution added by the stochastic model is over-predicted.

1. Introduction

The dynamical behavior of particles suspended in turbulent flows continues to receive attention because of its relevance to a wide range of applications, including liquid spray injection in gas turbines, rocket boosters, fluidized beds, pollutant dispersion, and sand/sediment transport. There are many computational approaches to model two-phase flows that differ mainly by the level of accuracy and computational cost. A simulation strategy of increasing interest consists in the coupling of Large Eddy Simulation (LES) of the fluid turbulence with discrete particle simulation (DPS) of the dispersed phase. This method typically requires tracking very large numbers of particles and can simulate practical processes more accurately than Reynolds-Averaged Navier-Stokes (RANS) approaches usually employed (Eulerian or Lagrangian).

An open issue, and the subject of this study, concerns the effect of subgrid turbulence on particle motion. In LES only the energy-containing eddies are resolved and the

† ONERA-CERT, 2 Avenue Edouard Belin 31500 Toulouse, France
‡ IMFT UMR CNRS/INPT/UPS, Avenue Camille Soula 31400 Toulouse, France
¶ Mechanical and Aerospace Engineering Department, Box 876106, Arizona State University, Tempe, Arizona 85257-6106, USA

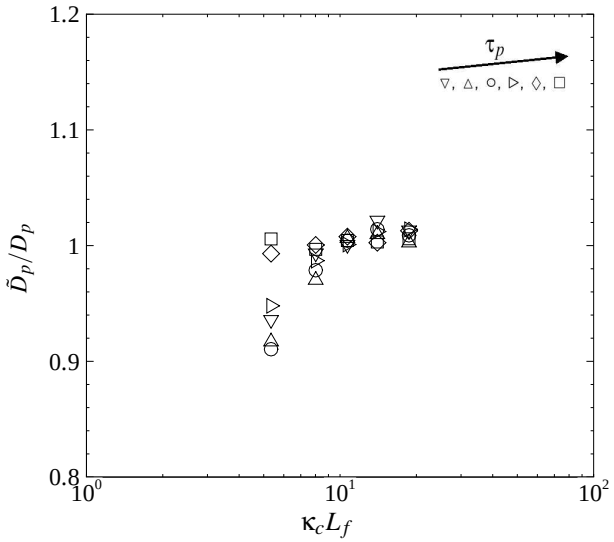

FIGURE 1. Particle dispersion coefficient measured in numerical simulations where the subgrid velocity is neglected, $\tilde{D}_p$, normalized by the value measured in DNS, D_p, as a function of cutoff wavenumber κ_c normalized by the fluid integral length scale. From Fede and Simonin (2006).

dissipative-scale effects are taken into account using a subgrid-scale (SGS) model. Investigations of the influence of subgrid turbulence on particle motion includes the studies made by Armenio *et al.* (1999), Yamamoto *et al.* (2001), Pozorsky *et al.* (2004), Shotorban and Mashayek (2005), and Fede and Simonin (2006). These studies have shown that for one-point particle statistics (particle dispersion, particle velocity fluctuations or the particle Lagrangian time scale), the subgrid turbulence has no significant effect on particle dynamics for parameter ranges in which the LES of the fluid flow is realistic (and accurate). This feature is illustrated in Fig. 1 and shows the particle dispersion coefficient measured in numerical simulations that do not include the effect of the subgrid velocity fluctuations normalized by the value measured in DNS. The ratio is plotted against the non-dimensional cutoff wavenumber $\kappa_c L_f$ (where L_f is the fluid integral length scale). The figure shows that for $\kappa_c L_f > 10$, the contribution of the subgrid turbulence in the dispersion mechanism is less than 2%.

While one-point statistics are negligibly affected for regimes in which the LES of the fluid should be accurate, for other phenomena such as particle segregation or inter-particle collisions, Fede and Simonin (2006) have shown that particle dynamics is much more influenced by subgrid fluid turbulence. Figure 2 shows a measure of particle segregation and illustrates that for a given range of subgrid Stokes numbers, defined as the ratio of τ_p, the particle response time, to $\delta\tau$, the subgrid characteristic time scale, the influence of subgrid fluid fluctuations accounts for different phenomena, i.e.,

- For $\tau_p/\delta\tau > 5$, the subgrid turbulence has no effect on particle segregation.
- For $\tau_p/\delta\tau \in [0.5;5]$, subgrid turbulence has a measurable effect on preferential concentration. In particular, Fig. 2 shows that the subgrid fluid velocity in this regime has a randomizing influence on the particle distribution.

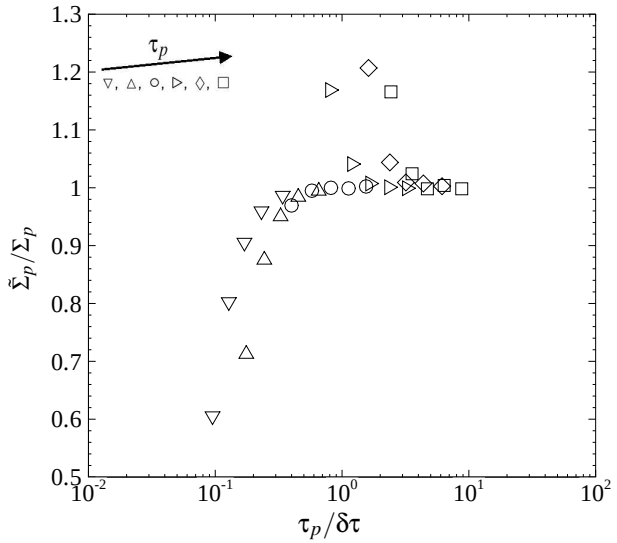

FIGURE 2. Particle segregation measured in numerical simulations where the subgrid velocity is neglected $\tilde{\Sigma}_p$ normalized by the value measured in DNS Σ_p with respect to the subgrid Stokes number $\tau_p/\delta\tau$. From Fede and Simonin (2006).

- For $\tau_p/\delta\tau < 0.5$, subgrid turbulence is very important since it comprises the dominant effect leading to preferential concentration.

The interpretation of these results in the frame of LES is that for $\tau_p/\delta\tau > 0.5$, the subgrid turbulence can be modeled using a stochastic Lagrangian approach. Moreover, if the LES is well-resolved ($\kappa_c L_f > 10$) and $\tau_p/\delta\tau > 5$, then subgrid model accounting for the influence of the unresolved fluid velocity on particle motion is not needed. In contrast, for $\tau_p/\delta\tau < 0.5$, one-point stochastic Lagrangian models appear ill-suited and other approaches are required (e.g., see Shotorban and Mashayek (2005)).

2. Modeling approach for the subgrid fluid velocity along inertial particle path

The instantaneous fluid velocity $u_{f,i}$ is decomposed as

$$u_{f,i} = \tilde{u}_{f,i} + \delta u_{f,i}, \tag{2.1}$$

where $\delta u_{f,i}$ is the subgrid contribution and $\tilde{u}_{f,i}$ is the filtered fluid velocity.

2.1. *General form of the Langevin equation along an inertial particle trajectory*

To establish the Langevin equation, we write the increment of the full fluid velocity along a fluid element trajectory as

$$u_{f,i}(\mathbf{x}+\mathbf{u}_f\Delta t, t+\Delta t) - u_{f,i}(\mathbf{x},t) = \left[-\frac{1}{\rho_f}\frac{\partial p}{\partial x_i} + \nu_f \frac{\partial^2 u_{f,i}}{\partial x_j \partial x_j}\right]\Delta t,$$

which corresponds to the discrete-in-time representation of the Navier-Stokes equations for incompressible flows where gravity is neglected. Using (2.1),

$$u_{f,i}(\mathbf{x}+\mathbf{u}_f\Delta t,t+\Delta t)-u_{f,i}(\mathbf{x},t)=\left[-\frac{1}{\rho_f}\frac{\partial\tilde{p}}{\partial x_i}+\nu_f\frac{\partial^2\tilde{u}_{f,i}}{\partial x_j\partial x_j}\right]\Delta t + \left[-\frac{1}{\rho_f}\frac{\partial\delta p}{\partial x_i}+\nu_f\frac{\partial^2\delta u_{f,i}}{\partial x_j\partial x_j}\right]\Delta t. \tag{2.2}$$

By analogy to Pope (1994) for single-phase turbulence and Simonin *et al.* (1993) for particulate flows, we write the contribution of the subgrid fluid velocity along an inertial particle trajectory as

$$u_{f,i}(\mathbf{x}+\mathbf{u}_p\Delta t,t+\Delta t)-u_{f,i}(\mathbf{x},t)=\left[-\frac{1}{\rho_f}\frac{\partial\tilde{p}}{\partial x_i}+\nu_f\frac{\partial^2\tilde{u}_{f,i}}{\partial x_j\partial x_j}\right]\Delta t + G_{fp,ij}\,(u_{f,j}-\tilde{u}_{f,j})\,\Delta t+(u_{p,j}-u_{f,j})\,\frac{\partial\tilde{u}_{f,i}}{\partial x_j}\Delta t+H\delta W_i, \tag{2.3}$$

where $\mathbf{u}_p$ is the particle instantaneous velocity, $G_{fp,ij}$ is a second-order tensor having the dimensions of frequency, δW_i is a Wiener process, and H is the intensity of the random contribution.

In the frame of LES, the contribution of the filtered fluid velocity is given by (see, for example, Sagaut (2002))

$$\frac{\partial\tilde{u}_{f,i}}{\partial x_i}=0 \tag{2.4}$$

$$\frac{\partial\tilde{u}_{f,i}}{\partial t}+\tilde{u}_{f,j}\frac{\partial\tilde{u}_{f,i}}{\partial x_j}=-\frac{1}{\rho_f}\frac{\partial\tilde{P}}{\partial x_i}+\nu_f\frac{\partial^2\tilde{u}_{f,i}}{\partial x_j\partial x_j}-\frac{\partial\tau_{ij}}{\partial x_j}, \tag{2.5}$$

where $\tau_{ij}=\widetilde{u_{f,i}u_{f,j}}-\tilde{u}_{f,i}\tilde{u}_{f,j}$ is the subgrid-scale stress tensor. We rewrite (2.5) in terms of velocity increment as

$$\left[-\frac{1}{\rho_f}\frac{\partial\tilde{P}}{\partial x_i}+\nu_f\frac{\partial^2\tilde{u}_{f,i}}{\partial x_j\partial x_j}\right]\Delta t=\tilde{u}_{f,i}(\mathbf{x}+\tilde{\mathbf{u}}_f\Delta t,t+\Delta t)-\tilde{u}_{f,i}(\mathbf{x},t)+\frac{\partial\tau_{ij}}{\partial x_j}\Delta t\,. \tag{2.6}$$

Hence, (2.3) becomes

$$u_{f,i}(\mathbf{x}+\mathbf{u}_p\Delta t,t+\Delta t)-u_{f,i}(\mathbf{x},t)=\tilde{u}_{f,i}(\mathbf{x}+\tilde{\mathbf{u}}_f\Delta t,t+\Delta t)-\tilde{u}_{f,i}(\mathbf{x},t) + \frac{\partial\tau_{ij}}{\partial x_j}\Delta t+(u_{p,j}-u_{f,j})\,\frac{\partial\tilde{u}_{f,i}}{\partial x_j}\Delta t+G_{fp,ij}\delta u_{f,j}\Delta t+H\delta W_i$$

and finally we obtain the following Langevin equation for the subgrid fluid velocity increment along an inertial particle path:

$$\delta u_{f,i}(\mathbf{x}+\mathbf{u}_p\Delta t,t+\Delta t)-\delta u_{f,i}(\mathbf{x},t)=-\delta u_{f,j}\frac{\partial\tilde{u}_{f,i}}{\partial x_j}\Delta t+\frac{\partial\tau_{ij}}{\partial x_j}\Delta t+G_{fp,ij}\delta u_{f,j}\Delta t + H\delta W_i\,. \tag{2.7}$$

In the right-hand side of the above equation, the first and second terms are exact and can be computed from the filtered fluid velocity field. In contrast, the third and fourth contributions are not closed and will be detailed in the following section.

2.2. *Closure of the Langevin equation*

The closure of (2.7) requires a model for the tensor $G_{fp,ij}$ and the intensity of the random contribution H. The expression of H can be derived using the Lagrangian structure function of the subgrid fluid velocity, $\delta\mathcal{R}_L(\tau)$, defined by

$$\delta\mathcal{R}_L(\tau) = \left\langle [\delta u_{f,i}(t_0+\tau) - \delta u_{f,i}(t_0)]\,[\delta u_{f,j}(t_0+\tau) - \delta u_{f,j}(t_0)] \right\rangle \tag{2.8}$$

For $\tau_K < \tau < \tau_L$, the Lagrangian structure function has a linear evolution Pope (1994) and is linked to the subgrid dissipation via

$$\delta\mathcal{R}_{L,ij}(\tau) = C_0^* \delta\varepsilon_f \tau \delta_{ij}, \tag{2.9}$$

where δ_{ij} is the Kronecker delta, C_0^* is the Kolmogorov constant, and $\delta\varepsilon_f$ is the subgrid fluid velocity dissipation. If we build the Lagrangian structure function using the Langevin equation (2.7), we obtain $\delta\mathcal{R}_{L,ij}(\tau) = H^2\tau\delta_{ij}$ leading to

$$H = \sqrt{C_0^* \delta\varepsilon_f}\,. \tag{2.10}$$

The numerical value of the Kolmogorov constant C_0^* is discussed in Section 3.4.

In (2.7) the only degree of freedom is the second-order tensor $G_{fp,ij}$. As previously discussed, this tensor has the physical dimensions of frequency. In the case of homogeneous isotropic turbulence, the following spherical form is adopted:

$$G_{fp,ij} = -\frac{1}{\delta\tau}\delta_{ij}. \tag{2.11}$$

In the present study the characteristic time scale $\delta\tau$ is given by a *consistency relation* that forces the Langevin equation to be consistent with the standard LES approach in terms of the subgrid kinetic energy. In particular, in the frame of standard LES, the transport equation of the subgrid kinetic energy $\delta q_f^2 = \delta\widetilde{u_{f,i}\delta u_{f,i}}/2$ is†

$$\begin{aligned}\frac{\partial \delta q_f^2}{\partial t} + \tilde{u}_{f,j}\frac{\partial \delta q_f^2}{\partial x_j} = &-\frac{1}{2}\frac{\partial}{\partial x_j}[\delta u_{f,j}\widetilde{\delta u_{f,i}\delta u_{f,i}}] \\ &+ \delta u_{f,i}\widetilde{\frac{\partial \tau_{ij}}{\partial x_j}} - \delta u_{f,i}\widetilde{\delta u_{f,j}\frac{\partial \tilde{u}_{f,i}}{\partial x_j}} - \delta\varepsilon_f,\end{aligned} \tag{2.12}$$

with the subgrid fluid dissipation given by,

$$\delta\varepsilon_f = \nu_f \widetilde{\frac{\partial \delta u_{f,i}}{\partial x_j}\frac{\partial \delta u_{f,j}}{\partial x_i}}\,. \tag{2.13}$$

For fluid elements, i.e., $\mathbf{u}_p = \mathbf{u}_f$, we equate (2.7) and (2.11) to derive the following transport equation for the subgrid kinetic energy:

$$\begin{aligned}\frac{\partial \delta q_f^2}{\partial t} + \tilde{u}_{f,j}\frac{\partial \delta q_f^2}{\partial x_j} = &-\frac{1}{2}\frac{\partial}{\partial x_j}\left\langle \delta u_{f,j}\delta u_{f,i}\delta u_{f,i}\right\rangle \\ &+ \left\langle \delta u_{f,i}\frac{\partial \tau_{ij}}{\partial x_j}\right\rangle - \left\langle \delta u_{f,i}\delta u_{f,j}\frac{\partial \tilde{u}_{f,i}}{\partial x_j}\right\rangle - \frac{2}{\delta\tau}\delta q_f^2 + \frac{3}{2}H^2,\end{aligned} \tag{2.14}$$

where $< \ . \ >$ is an averaging operator. Assuming that the average $< \ . \ >$ is equivalent to the filtering $\widetilde{\ .\ }$ we can equate (2.12) and (2.14). Finally, using $H = \sqrt{C_0^*\delta\varepsilon_f}$ we obtain

† assuming that the pressure-subgrid fluid velocity correlation can be neglected.

Reynolds number		Re_L	61
Fluid kinetic energy	$(m^2.s^{-2})$	q_f^2	$6.56\ 10^{-3}$
r.m.s fluid velocity $(=\sqrt{2q_f^2/3})$	$(m.s^{-1})$	u'_f	$6.61\ 10^{-2}$
Dissipation rate	$(m^2.s^{-3})$	ε_f	$16.3\ 10^{-3}$
Dissipation time scale $(=q_f^2/\varepsilon_f)$		τ_ε/τ_K	13.96
Integral length scale		L_f/L_b	0.11
Eulerian integral time scale		τ_E/τ_K	6.94
Lagrangian integral time scale		τ_L/τ_K	5.63
Kolmogorov time scale	(s)	τ_K	$28.8\ 10^{-3}$
Kolmogorov length scale		η_K/L_f	0.048
		$\kappa_{max}\eta_K$	2.01

TABLE 1. Turbulent fluid flow statistics computed in DNS with $N = 128^3$ mesh points.

the following consistency relation:

$$\delta\tau = \left[\frac{1}{2} + \frac{3C_0^*}{4}\right]^{-1} \frac{\delta q_f^2}{\delta\varepsilon_f}. \tag{2.15}$$

The relation (2.15) closes the Langevin equation in the sense that δq_f^2 and $\delta\varepsilon_f$ can be estimated from the filtered fluid velocity field in the frame of the LES approach. It must also be noted that we have not taken into account the effect of particle inertia, such as crossing trajectory effects, on the subgrid time scale $\delta\tau$. Such extensions are an important next step in the modeling.

2.3. *Evaluation of* δq_f^2 *and* $\delta\varepsilon_f$

In the frame of the Smagorinsky (1963) model, the subgrid dissipation may be approximated as

$$\delta\varepsilon_f = C_S\Delta^2|S|^3, \tag{2.16}$$

where C_S is the Smagorinsky constant (its value is discussed in Section 3.4), Δ is the filter width, $|S| = \sqrt{2S_{ij}S_{ij}}$ the modulus of the filtered strain tensor,

$$S_{ij} = \frac{1}{2}\left[\frac{\partial\tilde{u}_{f,i}}{\partial x_j} + \frac{\partial\tilde{u}_{f,j}}{\partial x_i}\right].$$

Yoshizawa (1982) proposed to compute the subgrid fluid kinetic energy according to

$$\delta q_f^2 = 2C_Y\Delta^2|S|^2, \tag{2.17}$$

where C_Y is the Yoshizawa constant detailed in Section 3.4. Combining (2.16) and (2.17) with (2.15) yields the following expression:

$$\delta\tau = \frac{1}{\beta|S|} \quad \text{with} \quad \beta = \left[\frac{1}{2} + \frac{3C_0^*}{4}\right]\frac{C_S}{2C_Y}. \tag{2.18}$$

3. Simulation overview

3.1. *Fluid flow simulation – DNS*

In this study the turbulence is homogeneous and isotropic and predicted using direct numerical simulation (DNS) of the incompressible Navier-Stokes equations for a fluid

Density	ρ_p/ρ_f	10 256	8 547	6 837	5 128	3 419	1 709
Diameter	d_p/η_K	0.1	0.1	0.1	0.1	0.1	0.1
Stokes number	τ_p/τ_K	5.34	4.46	3.58	2.70	1.81	0.91
Subgrid Stokes number	$\tau_p/\delta\tau$	3.78	3.16	3.54	1.91	1.28	0.64

TABLE 2. Particle properties and statistics with $\delta\tau/\tau_K = 1.41$.

of density $\rho_f = 1.17\ kg.m^{-3}$ and kinematic viscosity $\nu_f = 1.47\ 10^{-5}\ m^2.s^{-1}$. The computational domain is a cubic box of length $L_b = 0.128\ m$ and with periodic boundary conditions. Spectral forcing proposed by Eswaran and Pope (1988) is applied to obtain a statistically stationary turbulent flow. More details on the numerical schemes and methods can be found in Magnaudet *et al.* (1995) and Février *et al.* (2001). The main fluid properties of the turbulent flow are summarized in Table 1. The turbulent fluid kinetic energy and dissipation are computed from the three-dimensional spectrum $E(\kappa)$,

$$q_f^2 = \int_0^{+\infty} E(\kappa)d\kappa \quad , \quad \varepsilon_f = 2\nu_f \int_0^{+\infty} \kappa^2 E(\kappa)d\kappa. \tag{3.1}$$

The integral length scale is defined as $L_f = \int_0^{+\infty} f(r)dr$ where $f(r)$ is the fluid velocity longitudinal correlation function. The Reynolds number given in Table 1 is defined as

$$Re_L = \frac{u'_f L_f}{\nu_f}. \tag{3.2}$$

The Kolmogorov time and length scales are calculated from

$$\tau_K = \left(\frac{\nu_f}{\varepsilon_f}\right)^{1/2} \quad , \quad \eta_K = \left(\frac{\nu_f^3}{\varepsilon_f}\right)^{1/4}. \tag{3.3}$$

3.2. *Discrete particle simulation (DPS)*

This study is restricted to a dispersed phase composed of N_p solid, spherical, and identical particles ($N_p = 200\ 000$). Inter-particle collisions and turbulence modulation by the particles (two-way coupling) are neglected because of the low volumetric fraction considered ($\alpha_p = 1.37\ 10^{-5}$).

Neglecting gravity and assuming a large particle-to-fluid density ratio ($\rho_p/\rho_f \gg 1$), the forces acting on the particle are reduced to the drag. Hence, the single-particle equations of motion are

$$\frac{dx_{p,i}}{dt} = u_{p,i} \quad , \quad \frac{du_{p,i}}{dt} = -\frac{u_{p,i} - u_{f@p,i}}{\tau_p}, \tag{3.4}$$

where $x_{p,i}$ and $u_{p,i}$ are the i^{th} component of the particle position and velocity. The particle response time, τ_p, is defined as

$$\tau_p = \frac{\rho_p}{\rho_f}\frac{4}{3}\frac{d_p}{C_d}\frac{1}{|\mathbf{u}_p - \mathbf{u}_{f@p}|}, \tag{3.5}$$

where $u_{f@p,i}$ is the fluid velocity at the particle position (locally undisturbed by the particle), also referred to as the fluid velocity "seen" by the particle. As two-way coupling is not considered, the undisturbed fluid velocity is given by the DNS and evaluated at the particle position using cubic splines or the shape function method (see Balachandar

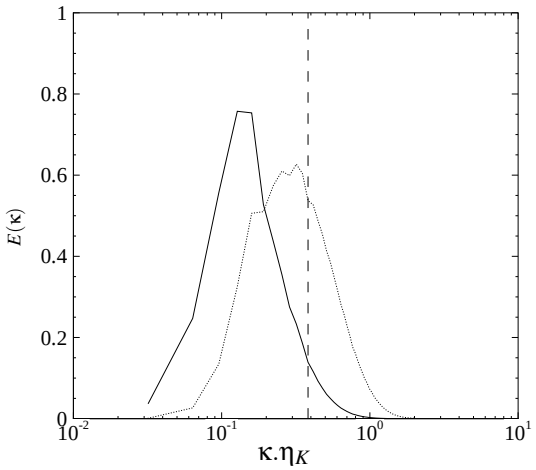

FIGURE 3. Energy (——) and dissipation (·····) spectra extracted from DNS. The dashed lines correspond to the filter wavenumber: $\kappa_c \eta_K = 0.38$.

and Maxey (1989)). The drag coefficient, C_d, is given by Schiller and Nauman (1935),

$$C_d = \frac{24}{Re_p}\left[1 + 0.15 Re_p^{0.687}\right], \tag{3.6}$$

where the particle Reynolds number is given by $Re_p = d_p|\mathbf{u}_p - \mathbf{u}_{f@p}|/\nu_f$ and the particle diameter, d_p, is much smaller than the Kolmogorov length scale of the undisturbed flow, $d_p \ll \eta_K$.

3.3. *Filtering procedure*

A spectral cutoff filter is used to separate the subgrid fluid velocity from the full instantaneous fluid velocity. Hence, the filtered fluid velocity field, $\tilde{u}_{f,i}$, is defined as

$$\tilde{u}_{f,i}(\mathbf{x},t) = FT^{-1}\left[\begin{cases} u^*_{f,i}(\kappa,t) & \text{if} \quad |\kappa| \in [\kappa_0, \kappa_c] \\ 0 & \text{otherwise} \end{cases}\right], \tag{3.7}$$

where κ_0 is the smallest resolved wavenumber ($\kappa_0 = 2\pi/L_b$), FT is the Fourier transform, κ_c the cutoff wavenumber, and $u^*_{f,i}$ is the fluid velocity field in Fourier space $u^*_{f,i}(\kappa,t) = FT\,[u_{f,i}(\mathbf{x},t)]$. The subgrid velocity field, $\delta u_{f,i}$, is obtained from

$$\delta u_{f,i}(\mathbf{x},t) = u_{f,i}(\mathbf{x},t) - \tilde{u}_{f,i}(\mathbf{x},t). \tag{3.8}$$

The filtered, $\tilde{u}_{f@p,i}$, and subgrid, $\delta u_{f@p,i}$, fluid velocity at the particle position are obtained by interpolation from the grid. Simulations have been performed for $\kappa_c = 12\kappa_0$ corresponding to $\kappa_c \eta_K = 0.38$ and $\kappa_c L_f = 8$. The position of the filter relative to the energy and dissipation spectra from the DNS is shown in Fig. 3.

Note that the filter does not modify prediction of the fluid flow in the DNS, i.e., the filtering is applied solely for computation of the fluid velocity at the particle position (prior to interpolation).

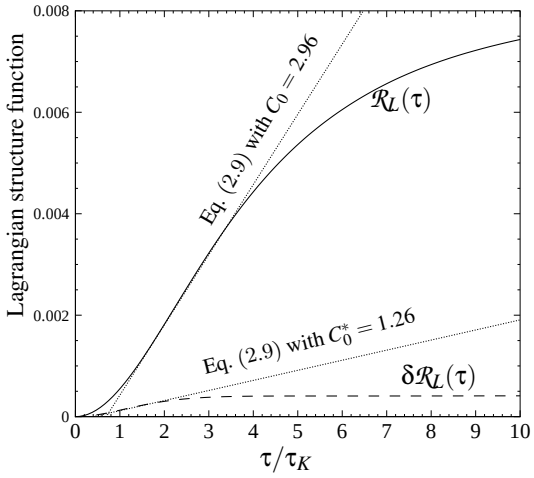

FIGURE 4. Lagrangian structure function measured in DNS for the full fluid velocity (——) and the subgrid fluid velocity (– – –), both measured using fluid element trajectories. The dotted lines correspond to the linear assumption (2.9), enabling determination of C_0^*.

3.4. *Langevin equation integration and constant determination*

The Langevin equation (2.7) is discretized using a first-order Euler scheme. The Wiener process is modeled as $\delta W_i = C\hat{\xi}$, where $\hat{\xi}$ is a random, normalized Gaussian variable. Using the property of the Wiener process, i.e., $\langle \delta W_i \delta W_i \rangle = \Delta t$, the constant C must be specified such that $C^2 = \Delta t$. Consequently, the numerical integration of the Langevin equation as performed together with the particle trajectory computation is accomplished as

$$\delta u_{f,i}^{n+1} = \delta u_{f,i}^{n} \left[1 - \frac{\Delta t}{\delta \tau}\right] - \left(\delta u_{f,j} \frac{\partial \tilde{u}_{f,i}}{\partial x_j}\right)^n \Delta t + \left(\frac{\partial \tau_{ij}}{\partial x_j}\right)^n \Delta t + \sqrt{C_0^* \delta \varepsilon_f \Delta t}\,\hat{\xi}, \tag{3.9}$$

with $\delta\varepsilon_f$ given by (2.16) and $\delta\tau$ by (2.18) both taken at time level n.

The model constants are important aspect of (3.9). For regimes corresponding to turbulent flows characterized by large scale-separation, the literature gives $C_0^* = 2.1$, $C_S = 0.18$, and $C_Y = 0.039$. In the present study, the DNS have been performed at a relatively low Reynolds number and with a limited separation of scales (see Fig. 3). Thus, the model constant are not universal and moreover, they depend on the filter width. For the present study, the constants are estimated from a single-phase DNS with fluid elements.

The value of the Kolmogorov constant C_0^* was computed using the Lagrangian structure function. In Fig. 4 are plotted the Lagrangian structure functions measured in the DNS for the full fluid velocity field $\mathcal{R}(\tau)$ and for the subgrid fluid velocity field $\delta\mathcal{R}_L(\tau)$. The simulations show that $\delta\mathcal{R}_L(\tau)$ follows a linear evolution for $\tau > \tau_K$, allowing extraction of the following value of the fitted "Kolmogorov constant":

$$C_0^* = 1.26.$$

As expected for $\mathcal{R}(\tau)$, the linear range is larger and $C_0 = 2.96$. This value is slightly different from the standard value 2.1, which is likely due to the low Reynolds number of the DNS.

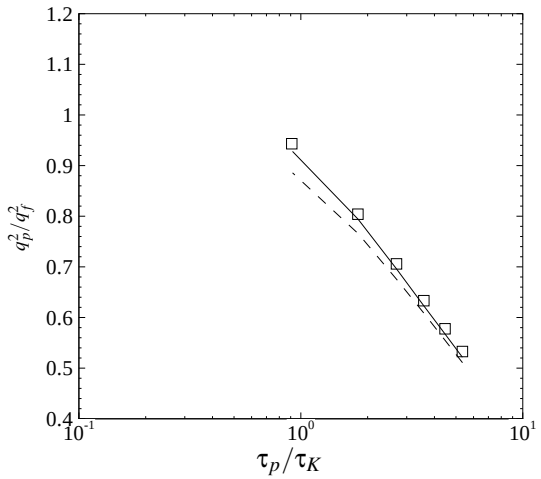

FIGURE 5. Particle kinetic energy normalized by the DNS kinetic energy. Results plotted are for ——: DNS + DPS; – – – : filtered DNS + DPS and symbols: "filtered DNS + Langevin equation" + DPS.

The Smagorinsky constant C_S is obtained from

$$C_S = \left\langle \frac{\nu_f \frac{\partial \delta u_{f,i}}{\partial x_j} \frac{\partial \delta u_{f,j}}{\partial x_i}}{\Delta^2 |S|^3} \right\rangle_{\text{over the domain}} \approx 2.2 \times 10^{-2} \tag{3.10}$$

and the Yoshizawa's constant C_Y with

$$C_Y = \left\langle \frac{\frac{1}{2} \delta u_{f,i} \delta u_{f,i}}{2\Delta^2 |S|^2} \right\rangle_{\text{over the domain}} \approx 1.1 \times 10^{-2}. \tag{3.11}$$

4. Results and discussion

4.1. *Methodology for model assessment*

In this study we have performed three different numerical simulations:

- **DNS + DPS**: in this case the fluid velocity used to solve (3.4) is given by the DNS. This numerical simulation is then our reference case.

- **Filtered DNS + DPS**: this corresponds to a simulation where the particle equation of motion (3.4) is advanced using the filtered fluid velocity $\tilde{\mathbf{u}}_{f@p}$ instead of $\mathbf{u}_{f@p}$. Hence, it represents an LES where the subgrid fluid velocity is neglected.

- **"Filtered DNS + Langevin equation" + DPS**: in this simulation the fluid velocity in (3.4) is $\mathbf{u}_{f@p} = \tilde{\mathbf{u}}_{f@p} + \delta\mathbf{u}_{f@p}$, where $\tilde{\mathbf{u}}_{f@p}$ is computed by filtering of the instantaneous DNS field before interpolation, and $\delta\mathbf{u}_{f@p}$ is predicted by (3.9).

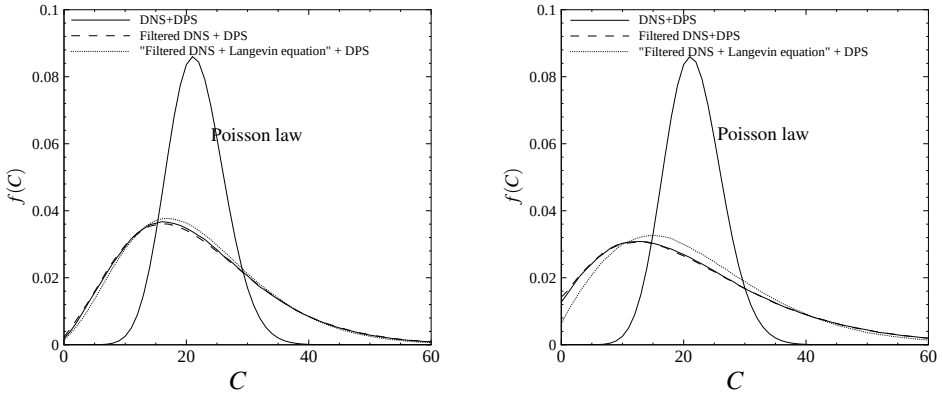

FIGURE 6. Particle concentration PDF for $\tau_p/\tau_K = 5.34$ (left panel) and $\tau_p/\tau_K = 2.70$ (right panel). Results shown are for —— : DNS + DPS; – – – : filtered DNS + DPS and ····· : "filtered DNS + Langevin equation" + DPS. The Poisson law corresponds to a random uniform distribution that has also been plotted.

4.2. *Particle kinetic energy*

Figure 5 shows the variation in the particle kinetic energy as a function of the particle Stokes number. We observe that for the *Filtered DNS + DPS*, the particle energy is underestimated for each case. This trend was expected because the filter applied (e.g., $\kappa_c L_f = 8$) is not in accordance with the limit criterion $\kappa_c L_f > 10$. Figure 5 also shows that the modification of the particle kinetic energy is more pronounced for light particles.

Figure 5 shows that the *"Filtered DNS + Langevin equation" + DPS* results match well the *DNS + DPS*, indicating that the proposed closure of the Langevin equation is consistent with the DNS for the kinetic energy.

4.3. *Particle segregation*

The effect of filtering on particle segregation is investigated using the probability density function (PDF) $f(C)$ of the particle concentration C. Particle segregation corresponds to $f(C)$, deviating from the Poisson law that describes a random uniform particle distribution. Figure 6 shows that in the present simulations there are strong effects of particle segregation.

Figure 6 also shows that the effect of filtering on the particle concentration is not significant (dashed vs. solid lines). The test case is therefore not relevant to assessing the Langevin model for accounting for segregation effects. Nevertheless, Fig. 6 shows that the stochastic model leads to a more uniform particle distribution. The figure shows that this trend, while expected given the form of the model, is overestimated.

5. Conclusion

A theoretical stochastic model has been derived to model the subgrid fluid velocity fluctuations along a particle path. The model closure has been derived in order that the Reynolds stresses provided by the model are identical to the ones of the standard LES approach. This yields a consistency equation that links the subgrid time scale with subgrid energy and dissipation. Following Smagorinsky and Yoshizawa, these quantities are expressed in term of the filtered fluid velocity field closing the stochastic model. The results presented in this study have shown that use of the model enables a match to

DNS data for the particle kinetic energy. In contrast, particle segregation is too strongly modified by the model which randomizes the particle distribution. Additionally, the test case used for model assessment in this work does not respect the criteria suggested by Fede and Simonin (2006) for a stochastic modelling of the subgrid fluid velocity. Hence, more numerical simulations with larger scale-separation should be performed to more accurately validate the model.

REFERENCES

Armenio V., Piomelli U. & Fiorotto V., 1999, Effect of the subgrid scales on particle motion, *Phys. Fluids*, **11** (10), 3030-3042.

Balachandar S. & Maxey M.R., 1989, Methods for evaluating fluid velocities in spectral simulations of turbulence, *J. Comput. Phys.*, **83**, 96-125.

Eswaran V. & Pope S.B., 1988, An examination of forcing in Direct Numerical Simulations of Turbulence, *Computers & Fluids*, **16**, 257-278.

Fede P. & Simonin O., 2006, Numerical study of the subgrid fluid turbulence effects on the statistics of heavy colliding particles, *Phys. Fluids*, **18**-045103.

Février P., Simonin O. & Legendre D., 2001, Particle dispersion and preferential concentration dependence on turbulent Reynolds number from Direct Numerical Simulation and Large Eddy Simulation of isotropic homogeneous turbulence, *Proc. 4th Int. Conference on Multiphase Flow*, ICMF-2000, New Orleans, USA.

Magnaudet J., Rivero M. & Fabre J., 1995, Accelerated flows past a rigid sphere or a spherical bubble. Part 1. Steady straining flow, *J. Fluid Mech.*, **284**, 97-135.

Pope S.B., 1994, Lagrangian PDF methods for turbulent flows, *Annu. Rev. Fluid Mech.*, **26**,23-63.

Pozorsky J., Apte S. V. & Raman V., 2004, Filtered particle tracking for dispersed two-phase turbulent flows, Center for Turbulence Research, in Proceedings of the Summer Program 2004.

Sagaut P., 2002, Large eddy simulation for incompressible flows, *Springer*.

Schiller L. & Nauman A., 1935, A drag coefficient correlation, *V.D.I. Zeitung*, **77**, 318-320.

Shotorban B. & Mashayek F., 2005, Modeling subgrid-scale effect on particles by approximate deconvolution, *Phys. Fluids*, **17**-08701.

Simonin O., Deutsch E. & Minier J.P., 1993, Eulerian prediction of the fluid/particle correlated motion in turbulent two-phase flows, *App. Sci. Res.*, **51**, 275-283.

Smagorinsky J., 1963, General circulation experiments with the primitive equations. I The basic experiment, *Mon. Weather Rev.*, **48**, 41-71.

Wang Q. & Squires K.D., 1996, Large eddy simulation of particle-laden turbulent channel flow, *Phys. Fluids*, **8** (5), 1207-1223.

Yamamoto Y., Potthoff M., Tanaka T., Kajishima T. & Tsuji Y., 2001, Large-eddy simulation of turbulent gas-particle flow in a vertical channel: effect of considering inter-particle collisions, *J. Fluid Mech.*, **442**, 303-334.

Yoshizawa A., 1982, A statistically-derived subgrid model for the large-eddy simulation of turbulence, *Phys. Fluids*, **25**, 1532-1538.